Chapter 11
Biomechanics of Single Cells and Cell Populations

Michael A. Teitell, Sheraz Kalim, Joanna Schmit, and Jason Reed

Abstract Cells form the basic unit of life. Their health and activities can be quantified by a multitude of biochemical and biophysical techniques that measure responses to external or internal stimuli. Many experimental approaches attempt to integrate molecular mechanisms with changes in the mechanical properties of cells, such as visocoelasticity and compliance, to link cell function with structure. An emerging view of cellular heterogeneity is that even within homogenous cell populations, individual cells may exhibit unique behavioral characteristics that deviate significantly from the population average. Here, several approaches for quantifying biophysical cellular responses are briefly reviewed and linked to specific underlying molecular mechanisms. We succinctly describe each approach and then elaborate on a new interferometer-based method for higher-throughput biophysical analysis of single cells within populations.

Cells adapt to changes in their microenvironment through coordinated molecular and mechanical activities. A variety of methods have been developed to interrogate cellular mechanical properties, such as viscoelasticity and deformability, mainly at the single cell level of analysis. These approaches include atomic force microscopy (AFM), [1–4], bio-microrheology (BMR), [5–7], magnetic twisting cytometry (MTC), [8], magnetic pulling cytometry (MPC), [9], micropipette aspiration,

M.A. Teitell (✉) and S. Kalim
Department of Pathology and Laboratory Medicine, UCLA, Los Angeles, CA, USA
e-mail: mteitell@ucla.edu

M.A. Teitell and J. Reed
California NanoSystems Institute, UCLA, Los Angeles, CA, USA

M.A. Teitell
Jonsson Comprehensive Cancer Center, Broad Center of Regenerative Medicine and Stem Cell Research, and Molecular Biology Institute, UCLA, Los Angeles, CA, USA

J. Schmit
Veeco Instruments, Inc., Tucson, AZ, 85706, USA

J. Reed
Department of Chemistry and Biochemistry, UCLA, Los Angeles, CA, USA

D. Ho (ed.), *Nanodiamonds: Applications in Biology and Nanoscale Medicine*,
DOI 10.1007/978-1-4419-0531-4_11,

[10, 11], microplate stretching rheometry, [12], optical stretching rheometry, [13], optical tweezers [14, 15], and many derivative methods

11.1 Approaches in Single Cell Biomechanics

AFM can measure dynamic changes in cell membrane rigidity, which may be used to infer underlying changes in signal transduction pathways or cytoskeletal components that can then be validated by standard molecular biology techniques, [2, 3, 16]. An AFM microcantilever is usually fabricated from silicon-based materials (Si, Si_3N_4) with a sharp tip at the terminal end, only hundreds of angstroms in size. When brought in contact with the cell surface, microcantilever deflections over time are detected by the motion of a laser reflected off the top surface of the cantilever. There are two predominant modes of AFM analysis for live cells, contact mode and tapping mode. In contact mode, the AFM tip is drawn to the sample surface until contact is made, followed by a sweep over the sample surface under constant deflection, controlled by a feedback piezoactuator. Because there is contact with the surface, the microcantilever spring constant is typically less than the elastic forces maintaining the cell's shape, and this value is usually close to 0.1 nN/mm [17, 18]. The feedback signal, recording the change in force needed to maintain a constant deflection, is processed as an image to reconstruct the appearance of the cell scanned at nanometer resolution. In tapping mode, the microcantilever oscillates above the sample surface, controlled by a piezoactuator. The deflection forces are processed into an image of the cell surface. The elastic or Young's modulus can be calculated from the deflection measurement and known spring constant of the microcantilever. The elastic modulus is a measure of the compliance of a cell. The lower the elastic modulus, the more prone the cell is to deformation.

Bio-microrheology (BMR) typically utilizes 100 nm-range fluorescent microbeads placed inside a cell as probes, rather than probing at the plasma membrane. In force-induced or active, BMR probe motion is controlled by an applied force, which can be from an external source, such as a magnet or laser tweezers, or by an intracellular ATP-dependent driver, such as the molecular motor proteins kinesin, dynein, and myosin [6]. In contrast, thermal or passive BMR is based on an extension of concepts from the Brownian motion of particles in simple liquids [5–7]. Microbead probe introduction is either passive, by endocytosis, or active, by microinjection or ballistic injection. The effect, if appreciable, on probe motion or location based upon the manner of probe introduction has not yet been systematically analyzed. In passive BMR, rapid, real-time video microscopy records small probe tracking displacements over time in the horizontal plane to evaluate the cell interior. Probe trajectories are used to calculate the time-dependent mean-squared displacement (MSD) of each probe to determine the rheological properties of the complex intracellular fluid microenvironment, such as the viscoelasticity. With step increases in stress, such as from step increases in an applied force, the creep compliance of each cell can be determined. MSD calculations can also be used to determine indi-

vidual probe motions, including trapped, subdiffusive, diffusive, combined diffusive and convective, and ballistic or purely convective particle trajectories, which can identify unique rheological subregions within single cells. Because the creep compliance is a measure of deformation with stress, this property can be used to calculate the interior elastic modulus and Young's modulus of a cell.

MTC and microplate stretching rheometry have been used in conjunction with chemical inhibitors, stimulants, or gene transfection to assess the role of cytoskeletal components, signal transduction pathways, and malignant cell transformation on cell rheologic properties. In MTC, ferromagnetic beads are attached to a cell membrane through a linked ligand that targets a specific membrane receptor. Using an applied magnetic field, the cell is stretched biaxially by the twisting of attached magnetic beads [19]. The bead rotation is measured by a magnetometer or optically [20] to calculate the elastic modulus of a cell. In microplate stretching rheometry, [21, 22], a single cell is grown between two borosilicate plates, one being rigid and the other flexible. As a cell deforms, due to changes in plate distance controlled by piezoelectric transduction, the deflection on the flexible plate, precalibrated for stiffness, is measured to calculate the viscoelastic properties of the cell.

Optical tweezers measure force displacement by focused laser beam trapping of beads attached to opposite ends of a single cell, which causes uniaxial stretching. Typically, the beads are a few microns in size and are attracted to a region with the highest photon density in a photon density gradient, created by a focused laser beam. [23]. Similarly, optical stretching uses counter-propagating divergent laser beams to trap and stretch individual cells [24]. However, optical stretching does not require pendant dielectric beads on the cell and uses two laser beams, which need not be focused. Cell stretching is achieved by asymmetric trapping of a cell, which imparts a resulting force, on the order of tens of pNs. Based on this stretching, stress profiles and deformability can be calculated for a cell.

In micropipette aspiration, [10], a suction pipette is used to aspirate a single cell and hold it firm at the pipette tip. The positive (suction) pressure required to do this is on the order of 100 Pa. By tracking the deflection of a bead attached to the cell opposite the aspirated end, the cortical tension, or the physical forces acting on the cell cortex that contribute to a defined cell shape, can be calculated.

11.2 Molecular Linkage to Cell Biomechanical Properties

Insights into global cell responses to specific stimuli can be gained by linking cell biomechanical properties with signal transduction, biochemical pathways, and the intracellular matrix, cytoskeleton, and cell membrane. For example, AFM has been used to investigate the relationship between Rho-A activation and cellular rigidity in human bronchial epithelial (HBE) cells. HBE cells transfected with a Rho-A inhibiting adenovirus that blocked normal Rho-A activity were significantly more deformable than control adenovirus infected cells [25]. These data seem logical since Rho-GTPases form a group of signaling proteins implicated in the regulation

of cell motility, cell morphology, cytoskeletal reorganization, and tumor progression [26]. Perhaps less intuitively, the biomechanical effects of steroids have also been explored at the single-cell level using AFM. Endothelial cells were treated separately with progesterone, estradiol, testosterone, aldosterone, and prednisolone, but only estradiol and aldosterone altered cell rigidity and shape, with aldosterone enhancing and estradiol lessening cell rigidity [27, 28]. These selective biomechanical activities would be harder to predict than the activities of the Rho-GTPases, but they do parallel the selective biochemical, physiological, and clinical effects of different steroid compounds [29]. The relationship between environmental factors and cell responses, such as plasma sodium and aldosterone exposure for endothelial cells, is of great interest in vascular inflammation and has also been studied with AFM [30, 31]. Endothelial cells treated with increasing levels of sodium alone showed no changes in cell rigidity. However, when treated with aldosterone, cell stiffness increased in constant sodium conditions. These findings extend the ongoing work [32] that may implicate endothelial cell dysfunction and increased cell rigidity in hypertension for patients with cardiovascular disease.

Cells in our bodies are constantly subjected to interstitial (non-vascular) fluid flow between cells, which is a common environmental feature of multicellular organism physiology. Studies of mouse fibroblasts using conditions that model interstitial fluid flow revealed increased cellular rigidity. Mouse fibroblasts subjected to shear stress also stiffened through increased actin reorganization and Rho-kinase activation [33]. Paralleling this result, BMR measurements of mouse fibroblasts [34] showed increased cellular viscosity and rigidity as a consequence of Rho-kinase activation. Mouse fibroblasts treated with LPA, a Rho-kinase activator, doubled in cell rigidity, further supporting the influence of Rho-kinase activation on cell rigidity and motility, and validating these links between cell physiology and biomechanics [35].

Biophysical methods have also helped to dissect the complexities of cellular structural organization. Recently, molecular complexes between nesprins and Sun proteins, known as LINC complexes, have been suggested as key structural elements in human cells, linking the nuclear lamina or membrane to the cytoskeleton. BMR studies in mouse fibroblasts [36] using ballistically introduced microparticles were tracked with and without transfection of known LINC complex inhibitors. The transfected cells were less rigid than control cells maintaining LINC complexes, suggesting a potential biomechanical component for, at least, some diseases associated with disruption of nuclear and cytoskeletal architecture. In contrast, micropipette aspiration studies [37] of neutrophil responses to specific microtubule inhibitors that disrupt the cytoskeleton revealed a minimal dependence on the microtubule network for cell structural integrity. Neutrophils treated with colchicine and paclitaxel, microtubule targeting drugs, increased cellular viscosity by 30%, and cortical tension by 18%. These increases in viscosity and tension were attributed to the presence of a compensatory F-actin polymerization response to disrupted microtubulin. This response to maintain cell structural integrity highlights the global interconnectedness of the cytoskeleton network and the compensatory processes that cells utilize to avoid mechanical collapse and death.

Density differences in nuclear and cytoplasmic regions of stem cells have been detected using micropipette aspiration, and linked to cytokine signaling [38] and nuclear import of various biomolecules [39, 40]. Nuclei in human embryonic stem cells were six times more rigid than the surrounding cytoplasm, yet deformed more readily than did fibroblasts derived from embryonic stem cell differentiation, implicating a changing biomechanical nuclear environment with cell differentiation [41]. Determinations of density differences between cells may be of great practical importance as well, because treatment efficacy has been linked to nuclear or cytoplasm density in some forms of leukemia [42].

Our own recent studies [6, 7, 43] measuring changes in viscoelasticity and membrane rigidity in single cells treated with a microtubule-dissociating drug have led to a further understanding of the compensatory actions of the cytoskeletal network. AFM studies showed that upon treatment with nocodazole, a microtubule depolymerizing agent, mouse fibroblasts exhibited local rigidity, rather than collapse and loss of structural integrity. The source for compensatory stabilization was likely a delicate and shifting balance between unstable, rapidly replaced tyrosinated microtubules (Tyr-MTs), stable detyrosinated long-term MTs (Glu-MTs), and the intermediate filaments of the cytoskeletal network. Our data suggested the existence of a pliable, so-called "transitional" mechanical state of a cell that can adjust to defects in the cytoskeletal network to avoid mechanical catastrophe and death. Detailed knowledge of this network action would likely be important for the design of drugs to rationally target specific components of the cytoskeleton, such as in therapy for cancer [44]. Consistent with these AFM results, BMR studies also showed a metastable mechanical transition phase that cells rely upon after treatment with nocodazole to avoid structural collapse. Overall, these two examples utilized different biophysical approaches to arrive at a complementary, mutually reinforcing model of a dynamic cytoskeletal compensatory response to maintain mechanical integrity.

11.3 Biomechanics for Numerous Cells in a Population- An Emerging Need?

Beyond determining single cell biomechanical responses to chemical and physical stimuli, or characterizing the structural properties of a cell, there is an increasing interest in utilizing viscoelastic and cell deformability changes to distinguish between cell types and possibly diseased cell states for potential clinical utility [45]. Recent studies of single cancer cells indicate a number of characteristic and reproducible changes in viscoelasticity and cell rigidity correlated with malignant transformation [13, 46, 47], the epithelial to mesenchymal transition (EMT), [48, 49], chemotherapy exposure, and tumor cell responses [50]. Measurements with optical tweezers of several malignant cell types reproducibly showed increased deformability compared with non-malignant cells, distinguishing a diseased state from a healthy state, based on differences in this cell mechanical property alone.

Biomechanical analysis of cancer cells may also provide useful information beyond traditional pathology and genetic-based characterizations and tumor grading. For example, increased cancer cell deformability may portend metastatic behavior and support similar conclusions from genetic or biochemical tests, increasing the confidence of adopting specific therapeutic strategies. Increased cell deformability from malignant transformation has been shown for pancreas epithelial, bladder epithelial, and mouse fibroblast cells. Panc-1, a pancreatic carcinoma cell line, showed enhanced deformability when treated with sphingosylphosphorylcholine (SPC), a lipid known to promote cancer metastasis, using microplate stretching. AFM studies comparing malignant and non-malignant human bladder epithelial cells showed that the Young's modulus of the non-cancerous cells was an order of magnitude higher than that of the cancerous cells [51]. A reduced viscoelastic modulus was also shown by AFM in simian virus 40-transformed, and H-Ras-transformed mouse fibroblasts, in comparison to non-transformed fibroblasts [52]. AFM studies of metastatic lung, breast, and pancreatic cancer cells from patient's pleural effusions showed that these cells were 80% more deformable than benign mesothelial cells ex vivo [53]. A biomechanical comparison of benign versus cancerous breast epithelial cells using AFM revealed increased elasticity for the cancer cells, with a Young's modulus almost double that of the benign cells [18]. More recently, disease progression in prostate cancer was studied by AFM. Three prostate cancer cell lines and a benign prostate epithelial cell line from a patient with prostate enlargement showed distinct Young's moduli, with the three cancer lines exhibiting reduced rigidity compared to the benign line [54]. Interestingly, the varied metastatic potential between these three cancer lines was reflected in the differences obtained for Young's moduli of these cells, and might be used to assess the likelihood for disease progression. Overall, mechanical differences between normal and cancer cells, or even between different cancer cells, suggests a detectable, quantifiable means for distinguishing between cell types, [47], diseased states, [13, 55], and possibly aggressive behavior based on cell viscoelasticity, rigidity, and deformation measurements. Data thus far, from a variety of different cancer types, both in vitro and ex vivo, using several biophysical methods suggests a general increase in deformability for cancer cells of many tissue types compared to the non-malignant cells from which they are derived.

Biomechanical studies of cancer and paired noncancerous cells has increased our understanding of cancer cell migration and motility, responses to stress, and signaling pathway activities [56]. However, recent advances in the molecular and cell biology of cancer suggest that not all cancer cells function equally, resulting in current uncertainty over the malignant potential of individual cancer cells within a population, and an uneasiness about the best clinical approach to eradicate certain types of malignancy. This current uncertainty can be overly simplified into two models of cancer. One model is a clonal evolution model [57], which asserts that normal cells acquire a cancerous phenotype through the acquisition of multiple, often characteristic genetic or epigenetic alterations. A central feature of this traditional model is that all of the cells forming a cancer have a similar potential for reinitiating the tumor within a rather narrow range of variability. Eradicating a

cancer using this model requires removing or killing all of the cancer cells from a patient. A competing model for cancer proposes the existence of relatively rare cells within a tumor, that are solely responsible for maintaining and reinitiating a tumor, rather than the bulk of the tumor cells themselves. These tumor-forming cells have been variously termed "cancer initiating cells" or "cancer stem cells" and a main focus of current research into cancer origins and therapy is focused on validating this model and identifying, characterizing, and eradicating these cells. This cancer stem cell hypothesis asserts that these cancer stem cells are solely capable of self-renewal and tumor propagation [58, 59]. In order to determine which of the competing models is most accurate for a given subtype of cancer, a large number of cells in a tumor would have to be prospectively analyzed one-by-one for their ability to self-renew and reinitiate a cancer. Bulk tumor cells and cancer stem cells could harbor unique biophysical properties for the same reasons that tumor versus non-malignant cells and cells of differing developmental origin can be identified using biomechanical profiling. Therefore, to potentially, prospectively identify rare cells in a population, such as cancer stem cells, or even to determine which cells in a population respond to certain treatments or altered environmental conditions, higher throughput methods for biomechanical analysis of live cells than currently exists are required. We and others are attempting to develop such new approaches.

11.4 Optical Profilometry for Higher Throughput Single Cell Biomechanical Profiling

We, along with the Gimzewski group at UCLA, devised a system that utilizes optical profilometry for nondestructive, near real-time quantification of biomechanical responses to force application or drugs [60, 61]. Optical profilometers, which are based on specialized microscopes with interferometric objectives, have been widely employed in the semiconductor, data storage, and MEMS fields for more than two decades [62]. These systems produce rapid, accurate, and reproducible nanoscale characterizations of surface roughness, form, film thickness, and more recently, dynamic behavior of MEMS and other moving devices. We have shown that with a proper configuration, optical profilers can sensitively and rapidly measure the biophysical properties of living biological systems.

Typically, optical profilers utilize light from a single source that is split, directed and reflected from a test object and a high quality reference surface to generate fringes from the interference of these two beams. Fringes created, as the objective is scanned along the optical axis that are detected by a camera, and analyzed to determine the shape of an object. In order to evaluate living cells, the system must be able to measure objects in fluid, which requires additional, specialized optical components to correct for the dispersive nature of the liquid medium. Also, the timescales of changing biomechanical properties can vary greatly, requiring a variety of measurement methodologies to maximize data, including strobed interferometry and video-rate deformation calculations. As discussed in the previous section,

the biophysical responses of individual cells can differ significantly from one another in a particular environment, making measurements of large numbers of cells in parallel an important requirement. This presents challenges, both in how to optimize the field-of-view for lateral resolution and how each image is analyzed, as the software intelligently tracks and logs information from many different cells simultaneously.

The optical profiler we used for live cell studies is, in principle, an optical microscope with a 20× 0.28NA Michelson interference objective that allows for the recording of not only lateral features with typical optical resolution (1.16 μm for the 20× objective) but also height dimensions of reflective objects below the scale of one nanometer. Live cells are maintained in an environmentally controlled chamber with a glass observation window. The Michelson interferometer is composed of a beam splitter, reference mirror and compensating fluid cell to adjust for optical path differences induced by fluid in the observation chamber. During each measurement, the objective head is scanned vertically from the reflective surface below the cells to a height of 40 μ above the surface, such that each point in the volume passes through focus. The interferometer is aligned so that the interference intensity distribution along the vertical scanning direction has its peak (best fringe contrast) at approximately the best focus position (Fig. 11.1).

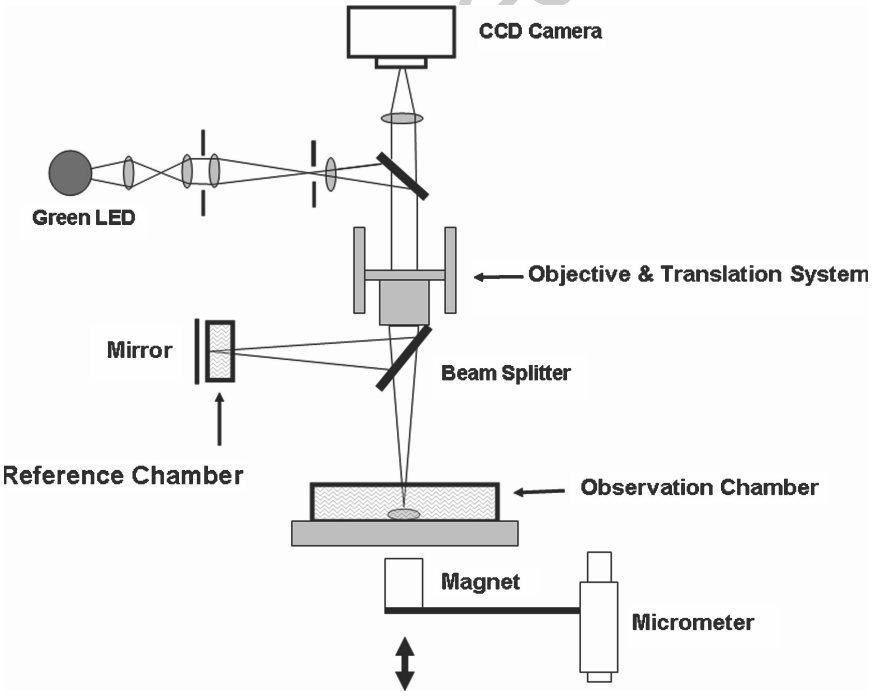

Fig. 11.1 Schematic of the interferometric profiler system used for live cell mechanical measurements

As shown in Fig. 11.2, three types of images can be obtained: a bright field microscopic image of the cell (*left*); a three-dimensional profile of microreflectors resting on the cell surface (*middle*); and an optical thickness image of the cell itself, which corresponds to the material density at every pixel (*right*). The interferometric height profile includes only the microreflector, since the cell-liquid interface is minimally reflective. Optical thickness, as discussed below, is calculated from the relative phase shift in the incident light as it propagates through the transparent film.

With this approach, the biomechanical properties of cells can be assessed in situ and in parallel using microindentation techniques. Samples are prepared for imaging by placing engineered magnetic microreflectors on top of cells and using these microreflectors as indentation probes for measuring nanometer displacements in cell height and position. Biomechanical properties such as the elasticity, viscocity and deformability of cells can be ascertained by imparting a magnetic field on the microreflectors (20pN – 20nN) to measure force displacement on the surface of the cell. Typically, contact indentation models, such as the Hertz model, are used to derive quantitative material properties of the cell from the force vs. indentation data. Other models can be used which account for adhesive properties of the cell surface, such as the Johnson-Kendall-Roberts (JKR) contact model [63]. A critical consideration for cell biomechanical studies is the dynamic range of the measurement technique. Mammalian cells exhibit a wide range of Young's moduli, from as soft as 10 Pa to as stiff as 100 kPa [64]. We estimate that the optical profiler can effectively measure samples with elastic moduli that vary from several Pa up to ~200 kPa, as currently configured. Live cells are known to exhibit complex frequency-dependent viscoelastic properties [21, 65, 66]. It is possible to use viscoelastic contact models to characterize the time-dependent elastic behavior of a cell, much like that routinely done for the study of soft polymers. In addition to the derived mechanical constants of the cell, interferometric imaging also provides direct biophysical data, such as cell thickness and position, for approximately ~1,000 cells, at any given time.

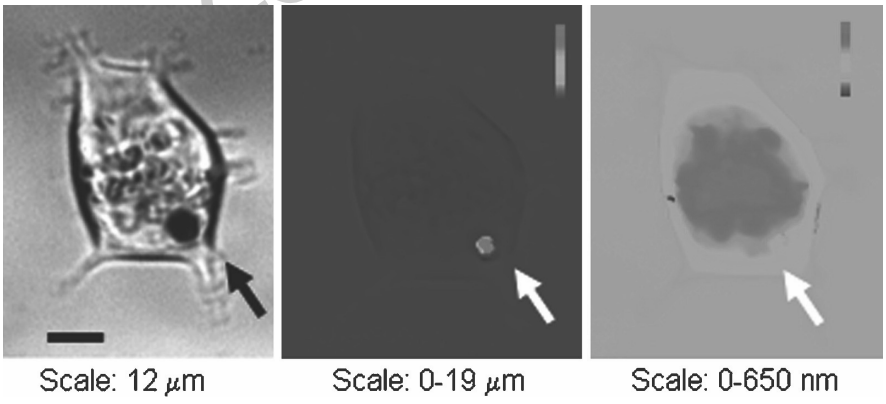

Fig. 11.2 Bright field (*left*) interferometric (*middle*) and optical thickness (right) images of an 8 micron microreflector (*arrows*) on a live NIH3T3 fibroblast in cell culture media

Optical thickness determined by interferometry is a well established technique to quantitatively and non-invasively measure local material density in transparent samples [67]. Figure 11.3 shows an optical thickness image of two live NIH3T3 mouse fibroblasts cells. The image shows details of each cell's internal structure, including the location of intracellular organelles. Cells are almost completely transparent in the visible spectrum, and the index of refraction of the fluid is close to the index of refraction of the interior, which does not allow much light to reflect off of the cell surface. Thus, almost all the light travels through the cell, and the signature of the material distribution within the cell is left on the measured phase. This signature is linear with the optical thickness of the cell because the whole wavefront traveling through the cell is interfered with the independent reference wavefront, and thus, this type of measurement is called quantitative phase imaging. Other quantitative phase imaging techniques are also being used for cell analyses, such as digital holography [68] and several interferometer variations [69]. The quantitative measurements of phase imaging avoids many issues of more traditional phase imaging techniques, such as Zernike phase contrast microscopy or differential interference contrast microscopy, that deliver only a qualitative measurement of cells.

Our initial studies [60, 61] evaluated the efficacy of using interferometry to profile live cells. We determined that the vertical motion in hundreds of NIH3T3 and HEK293T fibroblasts can be monitored simultaneously at a spatial resolution of <20 nm. Viscoelastic constants were determined by fitting the indentation curves to a time-dependent version of the three-factor model for a spherical indenter**.** For both cell types, the population viscoelastic constants were log-normally distributed. This result is in agreement with recent reports [64]. In contrast, most AFM/probe-based indentation studies have used small sample sizes ($n < 30$), and unlike optical profiling, do not have the sampling breadth to resolve the extended tail of the log-normal distribution. Failure to properly characterize this distribution can result

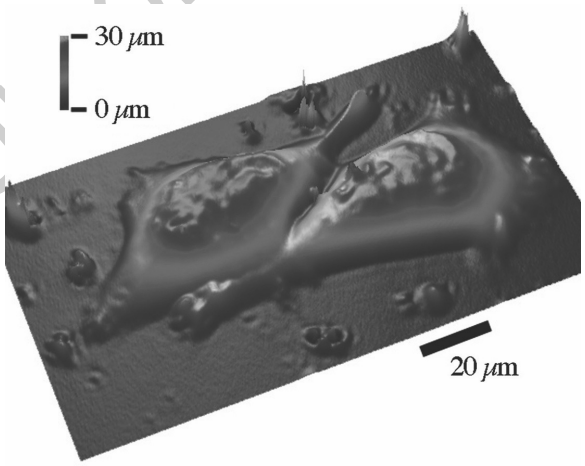

Fig. 11.3 Optical thickness image of live NIH 3 T3 cells in cell culture media

in erroneous conclusions when comparing experimental treatments or different cell types, especially when attempting to identify "outlier" cells that display distinct biophysical properties in a population. In addition, we achieved high throughput measurement of changes in viscoelastic behavior of NIH3T3 cells, when treated with cytochalasin-B, an actin depolymerizing drug. At low doses (0.1–1 μM), cytochalasin B does not produce large changes in the morphology of fibroblasts, although it does inhibit cell migration, [70, 71], and AFM indentation studies have reported minimal, if any, measurable change in Young's modulus [72]. In contrast, we determined that treated cells were more elastic, although their viscosity showed little or no decrease.

In a more recent study, the local redistribution of cell content was monitored as small indentions were made by highly magnetic probes, on the cell surface, using a rare earth magnet [61]. There was almost instantaneous redistribution of cell material, as a result of indentation on the surface of the cell, which was undetected with conventional optical microscopy alone. We analyzed the time-dependence of the content shift between specific regions of the cell by measuring the change in average optical thickness within four sub-regions of the cell body. The undriven regions responded at the same frequency as the driven regions, but with a temporal delay, as would be expected from a viscoelastic material. The amplitudes of motion of both the driven and undriven regions increased with time. Changes in local compliance were observed within 200s when force was applied cyclically to regions of the cell. It would be extremely difficult to measure these types of immediate viscoelastic parameters, at such a large scale, using conventional biophysical measurement techniques.

Our results show that optical profilometry achieves high throughput when measuring biomechanical properties using indentation normal to the cell surface. This represents a significant throughput advance over AFM, and other optical approaches, such as confocal microscopy or microfluidic optical stretchers, which cannot accurately measure mechanical properties of large arrays (hundreds to thousands) of cells simultaneously, with a single-cell specificity [72, 73]. The mechanical dynamic range and effective magnification of interferometric optical profiling equals or exceeds existing wide-field optical particle tracking techniques, [74], which implies that the two could be used in combination to conduct rapid, fully-3D mechanical probing of large arrays of live cells.

Acknowledgments Work on optical profilometry in the Teitell lab is generously supported by the UC Discovery/Abraxis Biosciences Biotechnology Award Bio07-10663. The authors thank Kayvan Niazi and Shahrooz Rabizadeh (Abraxis Biosciences) for encouragement and insightful discussions, and Daphne Weihs (Technion University), for critical reading and comments on the manuscript.

References

1. Benmouna F, Johannsmann D (2004) Langmuir 20:188–193
2. Dufrene YF (2008) Nat Rev Micro 6:674–680
3. Mahaffy RE, Park S, Gerde E, Kas J, Shih CK (2004) Biophys J 86:1777–1793

4. Mahaffy RE, Shih CK, MacKintosh FC, Käs J (2000) Phys Rev Lett 85:880
5. Crocker J, Hoffman B (2007) Meth Cell Biol 83:141–178
6. Weihs D, Mason TG, Teitell MA (2006) Biophys J 91:4296–4305
7. Weihs D, Teitell M, Mason T (2007) Microfluid Nanofluid 3:227–237
8. Gardel ML, Shin JH, MacKintosh FC, Mahadevan L, Matsudaira P, Weitz DA (2004) Science 304:1301–1305
9. Overby DR, Matthews BD, Alsberg E, Ingber DE (2005) Acta Biomaterialia 1:295–303
10. Hochmuth RM (2000) J Biomech 33:15–22
11. Hoffman BD, Massiera G, Van C, Kathleen M, Crocker JC (2006) Proc Natl Acad Sci USA 103:10259–10264
12. Suresh S, Spatz J, Mills JP, Micoulet A, Dao M, Lim CT, Beil M, Seufferlein T (2005) Acta Biomaterialia 1:15–30
13. Guck J, Schinkinger S, Lincoln B, Wottawah F, Ebert S, Romeyke M, Lenz D, Erickson HM, Ananthakrishnan R, Mitchell D, Kas J, Ulvick S, Bilby C (2005) Biophys J 88:3689–3698
14. Dao M, Lim CT, Suresh S (2003) J Mech Phys Solids 51:2259–2280
15. Svoboda K, Schmidt CF, Schnapp BJ, Block SM (1993) Nature 365:721–727
16. Muller DJ, Dufrene YF (2008) Nat Nano 3:261–269
17. Afrin R, Yamada T, Ikai A (2004) Ultramicroscopy 100:187–195
18. Li QS, Lee GYH, Ong CN, Lim CT (2008) Biochem Biophys Res Comm 374:609–613
19. Puig-De-Morales M, Grabulosa M, Alcaraz J, Mullol J, Maksym GN, Fredberg JJ, Navajas D (2001) J Appl Physiol 91:1152–1159
20. Bausch AR, Moller W, Sackmann E (1999) Biophys J 76:573–579
21. Desprat N, Richert A, Simeon J, Asnacios A (2005) Biophys J 88:2224–2233
22. Micoulet A, Spatz Joachim P, Ott Albrecht (2005) Chem Phys Chem. 6, 663–670.
23. Reece PJ (2008) Nat Photon 2:333–334
24. Guck J, Ananthakrishnan R, Mahmood H, Moon TJ, Cunningham CC, Kas J (2001) Biophys J 81:767–784
25. Wagh AA, Roan E, Chapman KE, Desai LP, Rendon DA, Eckstein EC, Waters CM (2008) AJP - Am J Physiol Lung cell Mol Physiol 295:L54–60
26. Sahai E, Marshall CJ (2002) Nat Rev Can 2:133–142
27. D'Ascenzo S, Millimaggi D, Di M Caterina, Saccani-Jotti G, BotrË F, Carta G, Tozzi-Ciancarelli MG, Pavan A, Dolo V (2007) Tox Lett. 169, 129-136.
28. Hillebrand U, Hausberg M, Lang D, Stock C, Riethmüller C, Callies C, Büssemaker E (2008) Pflugers Archiv 456:51–60
29. Miller VM, Mulvagh SL (2007) Trends Pharm Sci 28:263–270
30. Brown NJ (2008) Hypertension 51:161–167
31. Oberleithner H, Riethm ller C, Schillers H, MacGregor GA, de W Hugh E, Hausberg M (2007) Proc Natl Acad Sci USA 104, 16281–16286
32. Lee HW, Karam J, Hussain B, Winer B (2008) Curr Diab Rep 8:208–213
33. Lee JSH, Panorchan P, Hale CM, Khatau SB, Kole TP, Tseng Y, Wirtz D (2006) J Cell Sci 119:1760–1768
34. Kole TP, Tseng Y, Huang L, Katz JL, Wirtz D (2004) Mol Biol Cell 15:3475–3484
35. Sander EE, ten Klooster JP, van D Sanne, van d K Rob A, Collard JG (1999) J Cell Biol 147, 1009–1022
36. Stewart-Hutchinson PJ, Hale CM, Wirtz D, Hodzic D (2008) Exp Cell Res 314:1892–1905
37. Tsai MA, Waugh RE, Keng PC (1998) Biophys J 74:3282–3291
38. Kreis S, Munz GA, Haan S, Heinrich PC, Behrmann I (2007) Mol Can Res 5:1331–1341
39. Kutty RK, Chen S, Samuel W, Vijayasarathy C, Duncan T, Tsai J-Y, Fariss RN, Carper D, Jaworski C, Wiggert B (2006) Biochem Biophys Res Comm 345:1333–1341
40. Trompeter H, Schiermeyer A, Blankenburg G, Hennig E, Soling H (1999) J Cell Sci 112:4113–4122
41. Pajerowski JD, Dahl KN, Zhong FL, Sammak PJ, Discher DE (2007) Proc Natl Acad Sci USA 104:15619–15624
42. Valkov NI, Gump JL, Engel R, Sullivan DM (2000) Br J Haematol 108:331–345

43. Pelling AE, Dawson DW, Carreon DM, Christiansen JJ, Shen RR, Teitell MA, Gimzewski JK (2007) Nanomed: Nanotech. Biol & Med 3:43–52
44. Kopf-Maier P, Muhlhausen SK (1992) Chem-Biol Interact 82:295–316
45. Suresh S (2007) Nat Nano 2:748–749
46. Beil M, Micoulet A, von W Gotz, Paschke S, Walther P, Omary MB, Van V Paul P, Gern U, Wolff-Hieber E, Eggermann J, Waltenberger J, Adler G, Spatz J, Seufferlein T (2003) Nat Cell Biol 5, 803–811.
47. Elson E (1988) l. Ann Rev Biophys and Biophys Chem 17:397–430
48. Gupta GP, MassaguÈ J (2006) Cell 127:679–695
49. Thiery JP (2003) Curr Op Cell Biol 15:740–746
50. Lam WA, Rosenbluth MJ, Fletcher DA (2007) Blood 109:3505–3508
51. Lekka M, Laidler P, Gil D, Lekki J, Stachura Z, Hrynkiewicz AZ (1999) Eur Biophys J 28:312–316
52. Park S, Koch D, Cardenas R, Kas J, Shih CK (2005) Biophys J 89:4330–4342
53. Cross SE, Jin Y-S, Rao J, Gimzewski JK (2007) Nat Nano 2:780–783
54. Faria EC, Ma N, Gazi E, Gardner P, Brown M, Clarke NW, Snook RD (2008) Analyst 133:1498–1500
55. Liu J, Ferrari M (2002) Dis Markers 18:175–184
56. Makale M (2007) Birth Defects Res C Embryo Today 81(4) 329–343
57. Nowell P (1976) Science 194:23–28
58. Lapidot T, Sirard C, Vormoor J, Murdoch B, Hoang T, Caceres-Cortes J, Minden M, Paterson B, Caligiuri MA, Dick JE (1994) Nature 367:645–648
59. Park CH, Bergsagel DE, McCulloch EA (1971) J Natl Can Inst 46:411–422
60. Reed J, Frank M, Troke JJ, Schmit J, Han S, Teitell MA, Gimzewski JK (2008) Nanotechnology 19, 235101
61. Reed J, Troke JJ, Schmit J, Han S, Teitell MA, Gimzewski JK (2008) ACS Nano 2:841–846
62. Optical Inspection of Microsystems (2006) Osten W (Ed); CRC Press; Vol. 109
63. Johnson KL, Kendall K, Roberts AD (1971) Proc Royal Soc London a-Math and Phys Sci. 324:301–313
64. Balland M, Desprat N, Icard D, Fereol S, Asnacios A, Browaeys J, Henon S, Gallet F (2006) Phys Rev E 74
65. Rico F, Buscemi L, Trepat X, Garbulosa M, Rotger M, Farre R, Navajas D (2003) Eur Biophys J 32:306
66. Lenormand G, Millet E, Fabry B, Butler JP, Fredberg JJ (2004) J R Soc Interface 1:91–97
67. Davies HG, Wilkins MHF, Chayen J, Lacour LF (1954) Quart J Micro Sci 95:271–278
68. Marquet P, Rappaz B, Magistretti PJ, Cuche E, Emery Y, Colomb T, Depeursinge C (2005) Opt Lett 30:468–470
69. Popescu G, Ikeda T, Dasari RR, Feld MS (2006) Opt Lett 31:775–777
70. Rotsch C, Radmacher M (2000) Biophys J 78:520–535
71. Yahara I, Harada F, Sekita S, Yoshihira K, Natori S (1982) J Cell Biol 92:69–78
72. Cheezum MK, Walker WF, Guilford WH (2001) Biophys J 81:2378–2388
73. Carter BC, Shubeita GT, Gross SP (2005) Phys Biol 2:60–72
74. Fabry B, Maksym GN, Shore SA, Moore PE, Panettieri RA, Butler JP, Fredberg JJ (2001) J Appl Physiol 91:986–994